nature photonics

Article

https://doi.org/10.1038/s41566-025-01653-w

Space-time-topological events in photonic quantum walks

Received: 16 July 2024

Accepted: 28 February 2025

Published online: 4 April 2025

Check for updates

A list of authors and their affiliations appears at the end of the paper

Time is, figuratively and literally, becoming the new dimension for crystalline matter. In a key recent advance, temporal and spatiotemporal crystals that exhibit periodicity in time and space-time, respectively, were reported, with unique properties such as spectra containing gaps not only in energy but also in momentum. Conversely, the field of topological physics, which has led to celebrated discoveries such as topological insulators featuring protected conducting surface states with immunity to backscattering, has so far been based on the notion of energy gaps and spatial boundaries only. Fundamentally rethinking the role of time, which in contrast to space exhibits a unique unidirectionality called the 'arrow of time', thus promises a new dimension for topological physics, setting paradigms of time and space-time topology based on the topological properties of momentum and energy–momentum gaps. Indeed, previous work has shown simulations of states which arise through the topology of momentum gaps and localize at temporal interfaces. Here we enter this new dimension of time and space-time topology. First, using discrete-time quantum walks on synthetic photonic lattices in coupled optical fibre loops, we observe such time topological states. We find a time-topological invariant and establish its relation to the observed time topological states. Transcending the separate concepts of space and time topology, we then propose and implement a system with an energy–momentum gap and introduce the concept of space-time topology, leading to topological states that are localized in both space and time, thus forming space-time topological events. We demonstrate that these are associated with unique effects such as causality-suppressed coupling or the limited collapse of space-time localization. Our study provides a model of time and space-time topology, highlighting an interplay of momentum and energy gap topology with applicability beyond photonics. In the field of topological physics, we anticipate a new role of causality and non-Hermiticity inspired by time and space-time topology. These concepts further invite exploration of connections to other fields where the arrow of time plays an important role. Moreover, our results enable the topological shaping of waves in space and time, with applications in spatiotemporal wave control for imaging or communication and topological lasers, for example.

e-mail: alexander.szameit@uni-rostock.de

https://doi.org/10.1038/s41566-025-01653-w

Crystals are matter with the highest degree of spatial order, with their structure being arranged in spatially repeating patterns. Recently, this pillar of science has been fundamentally rethought[1]. As spatial crystals are defined by their periodicity in space, the highly active fields of temporal[2–4] and spatiotemporal[5–7] crystals refer to structures that repeat periodically in time and space-time, respectively. In photonics specifically, temporal crystals are also referred to as time-varying media or photonic time crystals[2], and they are reminiscent although distinct from Wilczek's proposal of time crystals[8,9]. In time crystals specifically, continuous time-translation symmetry is broken spontaneously, often as a result of (quantum) many-body interactions, whereas temporal crystals, as we consider them here, generally refer to any system with discrete time-translation symmetry only[2]. Rethinking the role of time also promises a new dimension for the celebrated field of topological physics, setting paradigms of time and space-time topology. Topological physics has become a unifying theme for diverse phenomena from seemingly distant fields, ranging from the celebrated quantum Hall effects for electrons[10,11] to equatorial ocean waves[12] and with promising applications such as topological quantum computation[13] based on the world line braiding of anyons[14], or topological lasers[15–17] enabled by photonic modes that are intrinsically resistant to scattering[18]. Yet, these topological features have so far relied on energy gap topology at spatial boundaries only, that is, the emergence of robust, long-lived states that reside within an energy gap while being localized at a spatial topological interface (Fig. 1a), which is the change of the relevant topological invariant in space[19,20]. This also includes Floquet topology[21], which considers such physics in time-periodic systems.

However, time is a new dimension for topology with fundamental differences from its spatial counterpart. Its unique unidirectionality, often called the 'arrow of time'[22], endows time with an intrinsic asymmetry which space does not exhibit. This asymmetry leads to strikingly different physics, for instance, such as time not supporting back-reflections but, instead, against all intuition, mandates the emergence of a unique notion of time reflections[23]. Correspondingly, unlike the familiar space topology, time topology may lead to topologically protected states that are localized at topological temporal interfaces (Fig. 1b, bottom), which are formed by the temporal change of a time-topological invariant. Previous work had shown simulations of such states[24]. Time topology is based not on energy but momentum gaps[24,25] (Fig. 1b): these are regions where the energies are imaginary-valued, leading to solutions decaying/growing in time, similar to evanescent waves in energy gaps, which decay in space. Momentum gaps can generically appear in driven and dissipative (non-Hermitian[26,27]) systems, implying an intrinsic connection between time topology and non-Hermiticity, unlike space topology for which non-Hermiticity is not generally necessary.

Here we demonstrate time-topological states localized at the temporal boundary of two photonic lattices with different momentum gap topology. We further introduce a time-topological invariant and establish a relation between this invariant and the observed time-topological states using a transfer matrix approach. Our experiments are based on a photonic lattice implemented through light propagation in coupled optical fibre loops[28–30]. The capability to modulate the optical properties of the fibre loops in time enables us to open and close momentum and energy gaps and to control their topology. Transcending the separate concepts of space and time topology, we introduce the notion of space-time topology by observing a space-time-topological event, that is, where a topological state localizes at a single point in space-time (Fig. 1c, bottom). The topological event emerges at the intersection of energy–momentum gapped photonic lattices whose topology is determined by a space-time-topological invariant that we introduce. It is of note that this topological state is localized in all available dimensions, including time, thus necessarily requiring the interplay of space and time in any causal system.

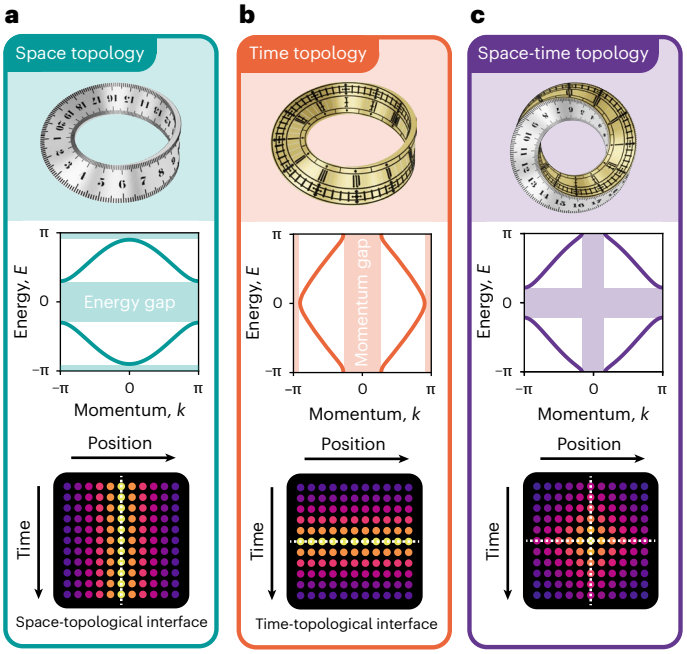

Fig. 1 | Space, time and space-time topology. a, Space topology (top) relies on energy bands separated by energy gaps (middle). The topology of energy gaps is associated with protected states that are localized at spatial interfaces (bottom), where the interface is represented by a dashed line, and brighter colours indicate a higher intensity. **b**, Time topology (top) relies on momentum bands separated by momentum gaps (middle). Time-topological states associated with the topology of momentum gaps may arise that are localized at temporal interfaces (bottom). **c**, Space-time topology (top) relies on bands that are gapped in energy and momentum (middle). Space-time-topological events, where topological states are localized at space-time interfaces (bottom).

Theory

We start by discussing the most fundamental scenario, that is, a one-dimensional two-band model, whose energy and momentum gaps can be independently controlled. In a second step, we deliberately close and open the momentum and energy gaps to control their corresponding topology. This enables our model to host topological states at temporal interfaces, which spectrally reside in the momentum gap, but also the well-established space topological counterparts, which are instead localized at spatial interfaces and reside in the energy gap. Finally, we realize a combined energy–momentum gap that features topological states that are localized at a single point in (1 + 1)-dimensional space-time, and as such constituting a topological event.

Our model is a time-varying implementation of the archetypal Su–Schrieffer–Heeger (SSH) model[31] with an additional gain–loss modulation that corresponds to a time-periodic drive of an imaginary on-site potential. The resulting evolution can be described in the framework of discrete-time quantum walks of single particles, as detailed in Supplementary Section 3, and then implemented via light propagation in coupled optical fibre loops as shown in Fig. 2. The experimental implementation uses a temporal encoding of pulse arrival times[32,33], creating a coupling of light between time bins that yields the dynamics of a photonic mesh lattice with a synthetic time (exhibiting the characteristic unidirectionality of time) and space dimension, as detailed in Supplementary Section 2.

The quantum walk describes the evolution of a quantum particle on discrete lattice positions x, which are coupled to neighbouring positions in a stepwise protocol along the time axis t. The dynamics are governed by the recursive evolution equations

https://doi.org/10.1038/s41566-025-01653-w

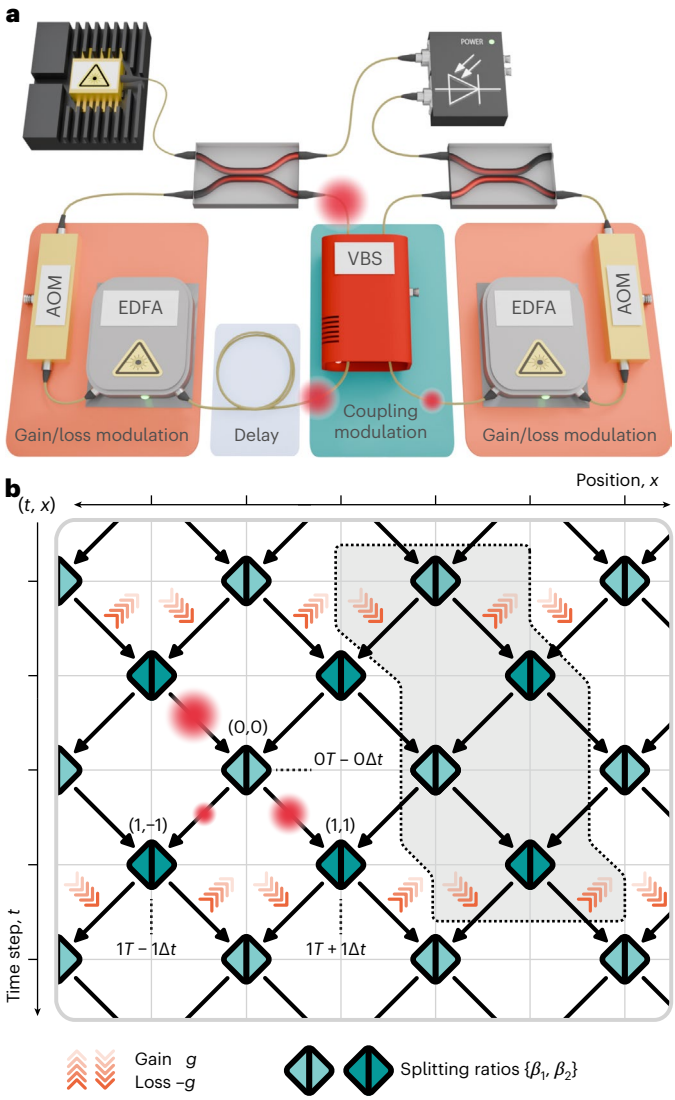

Fig. 2 | Experimental implementation of topological photonic lattices. **a**,**b**, Simplified experimental set-up for the realization of photonic lattices (**a**) and schematic of a photonic lattice (**b**). In **a**, two optical fibre loops are connected by a variable beamsplitter (VBS) that sets the coupling β. Acousto-optical amplitude modulators (AOMs) and erbium-doped fibre amplifiers (EDFA) enable a gain–loss modulation $\exp(\pm g)$. A pulse (red circle) that is coupled into the longer loop, splits up into two pulses that are delayed by $T \pm \Delta T$. They map to the photonic lattice in **b** where the average roundtrip delay T corresponds to time steps $t \to t+1$, and the relative delay within one roundtrip determines the position via multiples $x \times \Delta T$. In **b**, the implemented photonic lattices consist of a mesh lattice of beamsplitters and gain–loss modulations, with a four-time-step period and a two-step spatial periodicity. The resulting Floquet–Bloch unit cell is shaded in grey.

$$\begin{aligned} u_x^{t+1} &= \left[\cos(\beta)\, u_{x+1}^t + \mathrm{i}\sin(\beta)\, v_{x+1}^t\right] e^{\mathrm{i}\varphi_u} \\ v_x^{t+1} &= \left[\mathrm{i}\sin(\beta)\, u_{x-1}^t + \cos(\beta)\, v_{x-1}^t\right] e^{\mathrm{i}\varphi_v}, \end{aligned} \tag{1}$$

where u_x^t and v_x^t are the amplitudes of the spin-like degree of freedom at lattice point x and time step t, corresponding to, respectively, the left- and right-moving paths in the photonic lattice (Fig. 2b). The parameter $\beta(t,x)$ characterizes the splitting ratio of the beamsplitters and, thus, mediates the coupling between lattice positions and spins. The lattice parameters $\mathrm{Re}(\varphi_v)$ and $\mathrm{Im}(\varphi_v)$ are additional real and imaginary phase contributions, respectively, for each component v picked up during evolution. By appropriately choosing $\varphi_v(t,x)$ as a function of the spin $v \in \{u,v\}$, lattice position x and time t, all three types of topological bandgap may be obtained. A single pulse that is inserted into the longer loop splits into two pulses, which acquire different delays. The average delay T corresponds to the discrete time steps $t \to t+1$, whereas the relative pulse delays encode the position via $x \times \Delta T$. In this form of time-multiplexing, the combination of repeated splitting, delay and combination of pulses yields the photonic lattice dynamics (see Supplementary Section 2). The resulting photonic lattice is shown in Fig. 2b. The coupling alternates between β_1 and β_2 in a two-time-step fashion, thereby realizing the SSH model, being accompanied by a four-time-step gain–loss modulation $\varphi_u(t+4) = \varphi_u(t)$ with $[\varphi_u(0), \varphi_u(1), \varphi_u(2), \varphi_u(3)] = [ig, 0, 0, -ig]$, where g is the real gain–loss strength, which is antisymmetrically distributed on the spin-like degree of freedom, that is, $\varphi_v = -\varphi_u$.

The resulting energy spectra are shown in the bottom row of Fig. 1. Their calculation is detailed in Supplementary Sections 4 and 5. For $g = 0$, one obtains the Hermitian Floquet SSH model[34], which is gapped in energy (Fig. 1a). These energy gaps are ranges where the energy is real whereas the momentum is imaginary, leading to spatially decaying solutions called evanescent waves[35]. Note that in a crystal, momentum becomes the periodic quasimomentum due to discrete spatial translation symmetry[36], whereas here, in addition, energy likewise becomes the periodic quasienergy due to the discrete translation symmetry in time, as stated by Floquet theory[37–39]. For $g \neq 0$, that is, with the addition of non-Hermiticity, and $\beta_1 = \beta_2 = \pi/4$, there are no energy but only momentum gaps (Fig. 1b), that is, regions where the momentum is real whereas the energy is imaginary, leading to temporally growing and decaying solutions[2]. Note that in Floquet systems, such as the one considered here, the momentum gap condition also allows the real part of the energy to be $\pm\pi$. Finally, for $g \neq 0$ and $\beta_1 \neq \beta_2$, one can find an energy–momentum gap (Fig. 1c), where neither energy nor momentum are real[5].

The occurrence of gaps in the spectrum of allowed energies plays a major role in topological physics[19], as demonstrated by the celebrated topological states of the SSH model, which may also emerge here. On the basis of the eigenstates of the Bloch Hamiltonian, one can calculate a topological invariant, that is, an integer winding number that remains invariant under perturbations that admit certain symmetries[20]. Its calculation is based on integrating the phase of the eigenstates accumulated along the energy bands, as detailed in Supplementary Section 6. The so-called bulk-boundary correspondence[40,41] then assures the emergence of topological states localized at spatial topological interfaces, which are defined as a spatial change of this (spatial) winding number. Note that the winding number can only change upon closing the energy gap, which can here be achieved by altering the couplings $\beta_{1,2}$. In the following we will show that in the presence of momentum gaps, the topological description can be extended to enable the prediction of time-topological states as well as space-time-topological states.

Results

As a starting point, with the Hermitian Floquet SSH model, we experimentally realize a photonic lattice that is gapped in energy and verify the emergence of spatial topological states. All parameters relevant to our experiments are found in Supplementary Section 1. If the spatial winding number changes across the spatial interface one expects topological states localized at the interface. Our experiments agree with previous work[34,42], showing the emergence of a spatially localized state at the spatial interface (realized through a change in $\beta_{1,2}$) only when the aforementioned difference is non-zero (Fig. 3a, bottom). Conversely, for the trivial case of equal winding numbers across the interface, no topological state can be seen (Fig. 3a, top). Note that, owing to the imperfect mode overlap between the excitation and the topological interface state, propagating bulk modes are also visible on the right.

However, this situation changes when closing the energy gap while opening a momentum gap (Fig. 1b, middle) to approach the realm of time topology. Experimentally, we achieve this by matching the two

https://doi.org/10.1038/s41566-025-01653-w

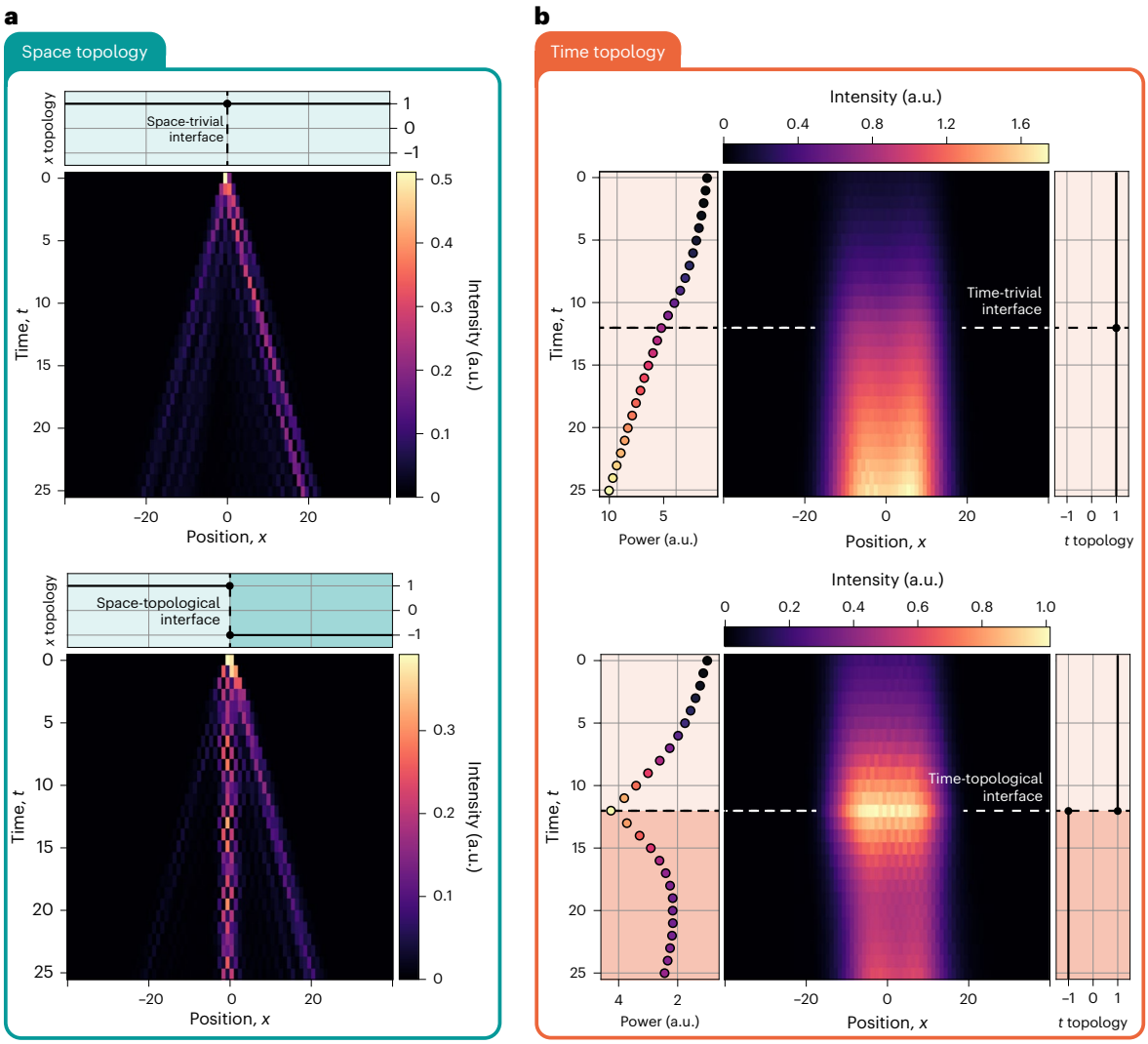

Fig. 3 | Experiments on space- and time-topological states. a, Light is injected at a topological (bottom) or trivial (top) spatial interface, that is, at the junction of two lattices with different or identical space-topological invariants, respectively. The familiar spatially localized topological state emerges only at the non-trivial interface. **b**, A spatially broad light field is injected. Here there is no spatial interface as in **a** but instead a topological (bottom) and trivial (top) temporal interface. A time-topological state that is localized in time emerges only in the case of a non-trivial temporal interface described by the time-topological invariant. The lattice parameters and calculation of the topological invariants are detailed in Supplementary Sections 1 and 5, respectively.

couplings $\beta_1 = \beta_2$ and applying a gain–loss modulation with $g = 0.1$, thus turning the system non-Hermitian. Importantly, its topological characterization must now be rethought: on the one hand, as the energy gap is now closed, the spatial winding number becomes ill-defined; on the other hand, however, there are now two momentum bands separated by the momentum gap. Momentum bands are potentially complex functions of real energies, just as energy bands are potentially complex functions of real momenta, as shown in Fig. 1. Their calculation is detailed in Supplementary Section 5. The eigenstates of the system may accumulate a geometric phase along these momentum bands, motivating the definition of a temporal winding number. The calculation of the temporal winding number is detailed in Supplementary Section 6. Moreover, using a transfer matrix approach, we show that the occurrence of time-topological states localized at temporal interfaces is predicted by changes of the temporal winding number in time (see Supplementary Sections 7 and 8). Such a time-topological interface state can clearly be observed in our experimental results (Fig. 3b, bottom), showing an exponential localization of light that is centred on the temporal interface (realized through a change in g) across which the invariant changes. Note that, unlike in the spatial case, there is some regrowth after the temporal interface due to a non-zero overlap with a growing mode (see Supplementary Sections 9 and 10). This regrowth may be suppressed and in theory even eliminated by minimizing the overlap to the growing mode and thus its excitation. The inherent growth and decay of the time-topological state points at the non-Hermitian nature of time topology. It is, however, distinct from conventional non-Hermitian topology as the time-topological invariant naturally arises from the consideration of momentum and not energy bands. This new type of topology is markedly different from concepts in which time is treated as a non-causal synthetic spatial dimension[43], and correspondingly falls into the category of traditional space topology without the unique aspects that arise from causality and momentum gap topology. We also note that related preliminary simulation results have indicated the existence of time-topological states not just in temporal but also in spatiotemporal crystals[44], without any evidence of space-time topology, however. An analytical derivation of the shape of the time-topological interface state that matches our experimental observations may be achieved by considering the projections of the left and right eigenstates before and after the interface (see Supplementary Sections 9 and 10). Conversely, for the trivial case

https://doi.org/10.1038/s41566-025-01653-w

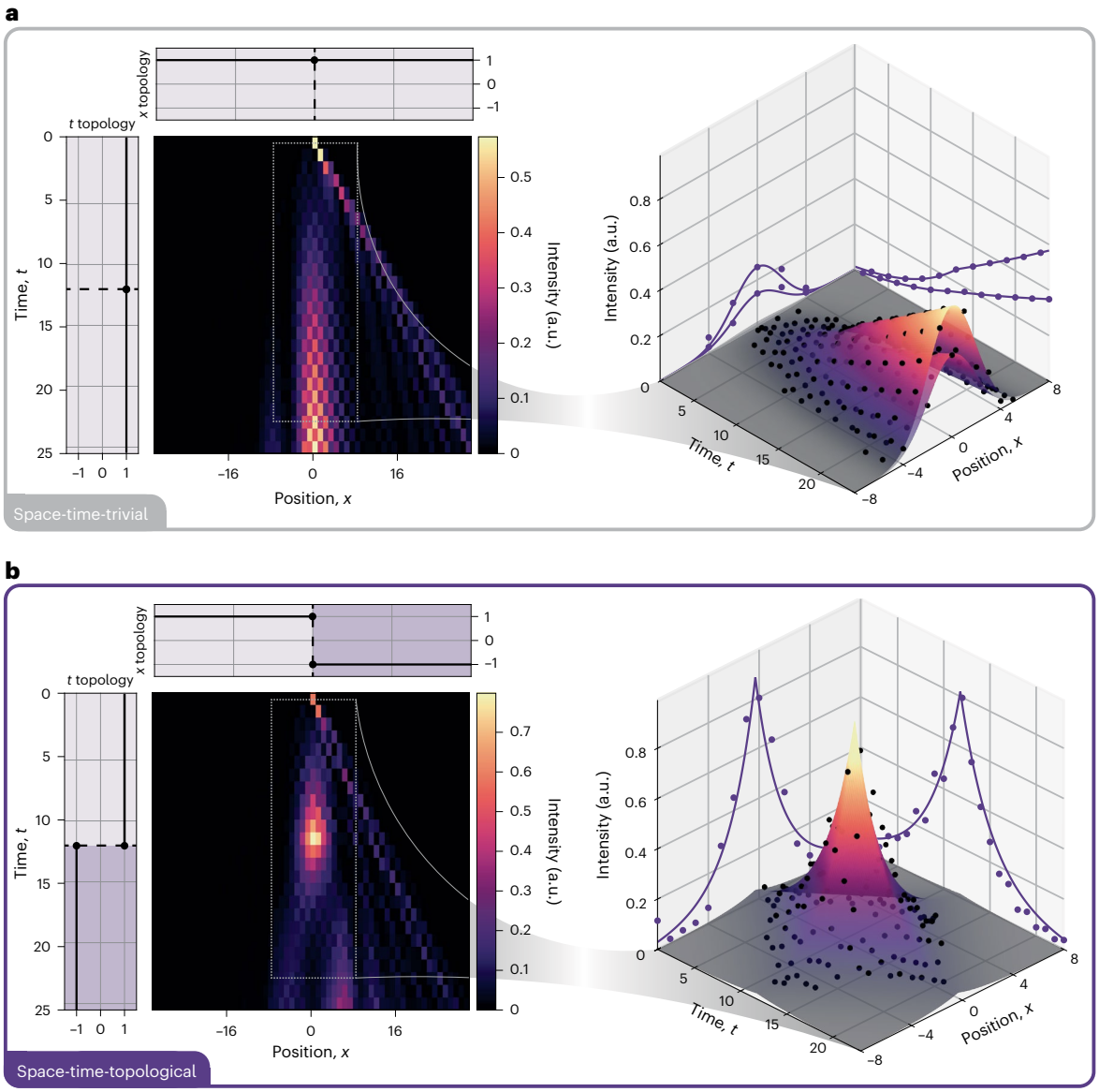

Fig. 4 | Observation of a space-time-topological event. a, In the space-time-trivial case, the light evolution shows neither exponential spatial nor any temporal localization at the intersection of a spatial and temporal interface. This is particularly evident for the data in the proximity of the intersection, where the evolution is described well by the fits of two growing modes of Gaussian shape that belong to different sublattices. **b**, At the intersection, a space-time-topological event, where a topological state localizes at a single point in space-time, can be seen. Light is injected at the spatial topological interface. Data in the proximity of the intersection are described well by a fit of a two-dimensional exponential decay, which is expected for the topological event. The lattice parameters and calculation of topological invariants are detailed in Supplementary Sections 1 and 5, respectively.

of equal temporal winding numbers across the temporal interface, no such state can be seen (Fig. 3b, top).

In the final step of our work, we are investigating a possible intertwinement of the familiar space topology with the notion of time topology. To this end, we probe whether a notion of space-time topology emerges in the presence of energy–momentum gaps. On the basis of the following results, we answer this question in the affirmative. By considering the product of the changes of the spatial and temporal winding number across their respective interfaces, we define a space-time-topological invariant for systems with combined energy–momentum gaps (see Supplementary Section 6). This invariant predicts the emergence of space-time-topological events, that is, where a topological state is exponentially localized on a single point in space-time. At this point, space-time regions, which are separated by a spatial and a temporal interface with different respective invariants across them, meet. We experimentally probe the light dynamics in the space-time-topological and -trivial cases, as shown in Fig. 4. In the trivial case, the light evolution shows neither the distinct exponential spatial localization nor any temporal localization (Fig. 4a). Note that the apparent remaining spatial localization in proximity to the injection point has no topological origin and can be explained via the complex band structure (see Supplementary Fig. 2): strongly growing modes inside energy regions with a constant real part of the energy (that is, non-dispersive) dominate the overall light distribution. In the topological case, the topological invariant correctly predicts the emergence of a light field that is exponentially localized along the time and space axes, while being located exactly at the designated interface crossing, thus forming the space-time-topological event (Fig. 4b).

This intertwinement of space-time with topology gives rise to unique effects with no analogue in traditional topology: for instance,

https://doi.org/10.1038/s41566-025-01653-w

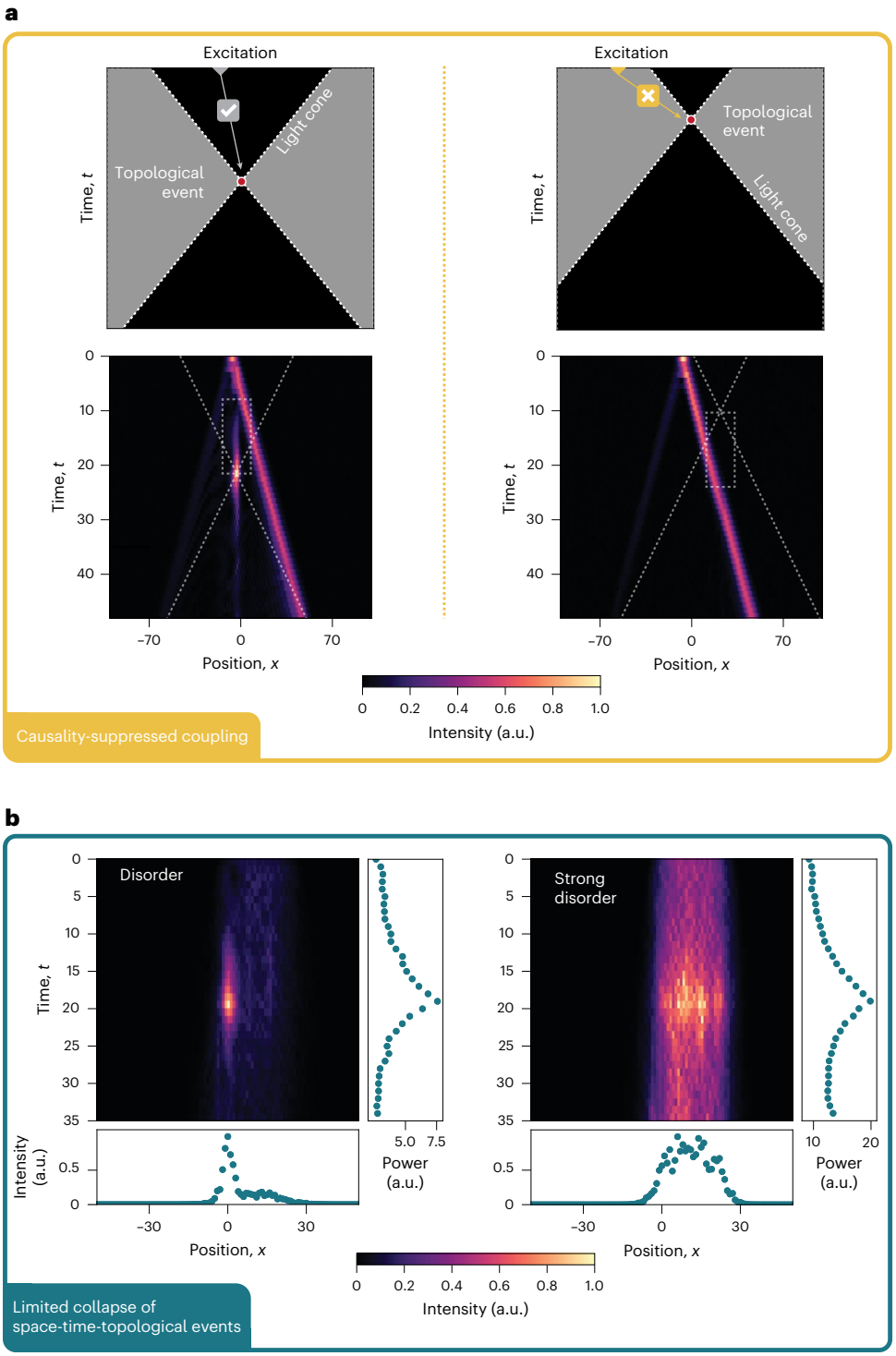

Fig. 5 | Experimental demonstration of causality-suppressed coupling and limited collapse of space-time-topological events. a, Coupling into the space-time-topological event is only possible from its past light cone (left), whereas coupling from its future light cone is completely suppressed due to causality (right), even for a finite overlap between excitation and the state. The light cones are shown as dashed lines. **b**, Shown here is the behaviour of space-time-topological events under phase disorder, that is, $\varphi_u(t,x) \rightarrow \varphi_u(t,x) + \delta(x)$ with $\delta(x)$ randomly chosen from an interval $[-\Delta\varphi,\Delta\varphi]$. The results are averaged over multiple disorder realizations. For moderate disorder (left, $\Delta\varphi = 0.2\pi$), the space-time localization remains robust. However, for strong disorder (right, $\Delta\varphi = 0.4\pi$) the limited collapse of the localization only occurs in space, whereas owing to the unique nature of the energy–momentum gap, which may close only partially, the temporal localization persists.

causality can suppress coupling into the topological event even when the excitation has a non-zero overlap with it. If an excitation is within its past light cone (Fig. 5a, left), the space-time-topological state will be excited when there is any overlap between the excitation and the profile of the state. However, if the excitation is not within the past light cone (Fig. 5a, right) of the space-time-topological event, the topological state will not be populated, no matter how large the overlap between the excitation and the state is. Hence, even though the overlap is approximately the same in both cases here, the coupling is allowed only when causality is obeyed, enabling a selective

excitation and hence endowing these states with an additional robustness against stray excitation unique among topological states. By contrast, in space topology, energy anywhere in the system will typically couple into and between topological states after some time, that is, impeding ideal topological protection and reducing their robustness in finite systems.

Furthermore, space-time-topological events exhibit unique behaviour under disorder. Owing to its distinct nature, it is possible for the energy–momentum gap to close only partially under disorder, leaving behind a momentum gap which maintains the temporal localization. This is shown in Fig. 5b, where it can be seen that, for moderate disorder (Fig. 5b, left), the space-time localization remains robust with only small distortions, whereas for strong disorder (Fig. 5b, right), the spatial localization collapses. However, this collapse is indeed limited to the spatial part of the space-time localization only, with the state remaining temporally localized. Such a limited collapse is markedly different from conventional topology, where closing the energy gap generally fully collapses all topological states, pointing at a new dimension of topological robustness where the collapse of topological localization may be limited to some but not all dimensions.

Conclusion

We have experimentally demonstrated time-topological states localized at temporal boundaries on the basis of the time topology of the momentum gap of a photonic lattice. The time topological states are predicted by a momentum-band-based winding number that we proposed. Owing to the growing and decaying nature of such states, their description naturally includes non-Hermiticity. We then transcend the separate notions of energy and momentum gap topology by demonstrating space-time-topological events, where topological states localize at a zero-dimensional space-time boundary. These topological events are predicted by a space-time-topological invariant that we defined. Their localization in all available dimensions, including time, necessitates a notion of space-time topology, bringing about unique features such as causality-suppressed coupling or the limited collapse of event states. Our results set the new paradigms of time and space-time topology, based on interconnections between the celebrated energy gap topology and the introduced notion of momentum gap topology. As such, we anticipate that our studies will have far-reaching implications. For the field of topological physics specifically, our work demonstrates a new avenue away from the conventional sole focus on spatial features of topological systems, towards the wider scope of space-time topology. The evident connection of time and space-time topology to non-Hermiticity also stimulates the possibility of a connection to the thriving field of non-Hermitian topology. Moreover, our work invites the exploration of how the concepts of time and space-time topology newly connect topological physics to other fields where the arrow of time plays an important role, such as thermodynamics. More generally, the ongoing efforts to engineer wave systems that are capable of ultrafast temporal modulations, with recent successes on implementing time interfaces in nonlinear optical media[45], ultracold atoms[46] and water waves[23], point towards a wide range of potential future platforms for time- and space-time-topological effects. In this vein, controlling momentum and energy gap topology may enable the topological shaping of various types of wave in space and time, with applications, for example, in spatiotemporal wave control for imaging or communication[47,48] and topological lasers[49].

Online content

Any methods, additional references, Nature Portfolio reporting summaries, source data, extended data, supplementary information, acknowledgements, peer review information; details of author contributions and competing interests; and statements of data and code availability are available at https://doi.org/10.1038/s41566-025-01653-w.

References

1. Wilczek, F. Crystals in time. *Sci. Am.* **321**, 28–36 (2019).
2. Galiffi, E. et al. Photonics of time-varying media. *Adv. Photonics* **4**, 014002 (2022).
3. Engheta, N. Four-dimensional optics using time-varying metamaterials. *Science* **379**, 1190–1191 (2023).
4. Wang, X. et al. Metasurface-based realization of photonic time crystals. *Sci. Adv.* **9**, eadg7541 (2023).
5. Sharabi, Y., Dikopoltsev, A., Lustig, E., Lumer, Y. & Segev, M. Spatiotemporal photonic crystals. *Optica* **9**, 585–592 (2022).
6. Caloz, C. & Deck-Léger, Z.-L. Spacetime metamaterials—part I: general concepts. *IEEE Trans. Antennas Propag.* **68**, 1569–1582 (2019).
7. Biancalana, F., Amann, A. & O'Reilly, E. P. Gap solitons in spatiotemporal photonic crystals. *Phys. Rev. A* **77**, 011801 (2008).
8. Wilczek, F. Quantum time crystals. *Phys. Rev. Lett.* **109**, 160401 (2012).
9. Zaletel, M. P. et al. Quantum and classical discrete time crystals. *Rev. Mod. Phys.* **95**, 031001 (2023).
10. Thouless, D. J., Kohmoto, M., Nightingale, M. P. & den Nijs, M. Quantized Hall conductance in a two-dimensional periodic potential. *Phys. Rev. Lett.* **49**, 405–408 (1982).
11. Eisenstein, J. P. & Störmer, H. L. The fractional quantum Hall effect. *Science* **248**, 1510–1516 (1990).
12. Delplace, P., Marston, J. B. & Venaille, A. Topological origin of equatorial waves. *Science* **358**, 1075–1077 (2017).
13. Nayak, C., Simon, S. H., Stern, A., Freedman, M. & Das Sarma, S. Non-Abelian anyons and topological quantum computation. *Rev. Mod. Phys.* **80**, 1083–1159 (2008).
14. Nakamura, J., Liang, S., Gardner, G. C. & Manfra, M. J. Direct observation of anyonic braiding statistics. *Nat. Phys.* **16**, 931–936 (2020).
15. Bandres, M. A. et al. Topological insulator laser: experiments. *Science* **359**, eaar4005 (2018).
16. Bahari, B. et al. Nonreciprocal lasing in topological cavities of arbitrary geometries. *Science* **358**, 636–640 (2017).
17. St-Jean, P. et al. Lasing in topological edge states of a one-dimensional lattice. *Nat. Photon.* **11**, 651–656 (2017).
18. Ozawa, T. et al. Topological photonics. *Rev. Mod. Phys.* **91**, 015006 (2019).
19. Hasan, M. Z. & Kane, C. L. Topological insulators. *Rev. Mod. Phys.* **82**, 3045–3067 (2010).
20. Asbóth, J. K., Oroszlány, L. & Pályi, A. *A Short Course on Topological Insulators: Band Structure and Edge States in One and Two Dimensions* Vol. 919 (Springer, 2016).
21. Kitagawa, T., Berg, E., Rudner, M. & Demler, E. Topological characterization of periodically driven quantum systems. *Phys. Rev. B* **82**, 235114 (2010).
22. Eddington, A. S. *The Nature of the Physical World: Gifford Lectures of 1927, An Annotated Edition* (Cambridge Scholars Publishing, 2014).
23. Bacot, V., Labousse, M., Eddi, A., Fink, M. & Fort, E. Time reversal and holography with spacetime transformations. *Nat. Phys.* **12**, 972–977 (2016).
24. Lustig, E., Sharabi, Y. & Segev, M. Topological aspects of photonic time crystals. *Optica* **5**, 1390–1395 (2018).
25. Reyes-Ayona, J. R. & Halevi, P. Observation of genuine wave vector (k or β) gap in a dynamic transmission line and temporal photonic crystals. *Appl. Phys. Lett.* **107**, 074101 (2015).
26. Ashida, Y., Gong, Z. & Ueda, M. Non-Hermitian physics. *Adv. Phys.* **69**, 249–435 (2020).
27. El-Ganainy, R. et al. Non-Hermitian physics and PT symmetry. *Nat. Phys.* **14**, 11–19 (2018).
28. Regensburger, A. et al. Parity–time synthetic photonic lattices. *Nature* **488**, 167–171 (2012).

29. Weidemann, S. et al. Topological funneling of light. *Science* **368**, 311–314 (2020).
30. Weidemann, S., Kremer, M., Longhi, S. & Szameit, A. Topological triple phase transition in non-Hermitian Floquet quasicrystals. *Nature* **601**, 354–359 (2022).
31. Su, W. P., Schrieffer, J. R. & Heeger, A. J. Solitons in polyacetylene. *Phys. Rev. Lett.* **42**, 1698–1701 (1979).
32. Ozawa, T. & Price, H. M. Topological quantum matter in synthetic dimensions. *Nat. Rev. Phys.* **1**, 349–357 (2019).
33. Yuan, L., Lin, Q., Xiao, M. & Fan, S. Synthetic dimension in photonics. *Optica* **5**, 1396–1405 (2018).
34. Kitagawa, T. et al. Observation of topologically protected bound states in photonic quantum walks. *Nat. Commun.* **3**, 882 (2012).
35. Born, M. & Wolf, E. *Principles of Optics: Electromagnetic Theory of Propagation, Interference and Diffraction of Light* (Cambridge Univ. Press, 1999).
36. Ashcroft, N. W. & Mermin, N. D. *Solid State Physics* (Holt, Rinehart and Winston, 1976).
37. Holthaus, M. Floquet engineering with quasienergy bands of periodically driven optical lattices. *J. Phys. B At. Mol. Opt. Phys.* **49**, 013001 (2015).
38. Yin, S., Galiffi, E. & Alù, A. Floquet metamaterials. *eLight* **2**, 8 (2022).
39. Rudner, M. S. & Lindner, N. H. Band structure engineering and non-equilibrium dynamics in Floquet topological insulators. *Nat. Rev. Phys.* **2**, 229–244 (2020).
40. Cedzich, C. et al. Bulk-edge correspondence of one-dimensional quantum walks. *J. Phys. A Math. Theor.* **49**, 21LT01 (2016).
41. Tanaka, Y. A constructive approach to topological invariants for one-dimensional strictly local operators. *J. Math. Anal. Appl.* **500**, 125072 (2021).
42. Malkova, N., Hromada, I., Wang, X., Bryant, G. & Chen, Z. Observation of optical Shockley-like surface states in photonic superlattices. *Opt. Lett.* **34**, 1633–1635 (2009).
43. Žlabys, G., Fan, C.-h., Anisimovas, E. & Sacha, K. Six-dimensional time–space crystalline structures. *Phys. Rev. B* **103**, L100301 (2021).
44. Segal, O. et al. Topology in photonic space-time crystals. In *Conference on Lasers and Electro-Optics* JW4A.4 (Optica Publishing Group, 2022); https://doi.org/10.1364/CLEO_AT.2022.JW4A.4
45. Zhou, Y. et al. Broadband frequency translation through time refraction in an epsilon-near-zero material. *Nat. Commun.* **11**, 2180 (2020).
46. Dong, Z. et al. Quantum time reflection and refraction of ultracold atoms. *Nat. Photon.* **18**, 68–73 (2024).
47. Shaltout, A. M., Shalaev, V. M. & Brongersma, M. L. Spatiotemporal light control with active metasurfaces. *Science* **364**, eaat3100 (2019).
48. Shen, Y. et al. Roadmap on spatiotemporal light fields. *J. Opt.* **25**, 093001 (2023).
49. Lyubarov, M. et al. Amplified emission and lasing in photonic time crystals. *Science* **377**, 425–428 (2022).

Joshua Feis [1,2,4], Sebastian Weidemann [1,4], Tom Sheppard [3], Hannah M. Price [3] & Alexander Szameit [1] ✉

[1]Institute of Physics, University of Rostock, Rostock, Germany. [2]Department of Engineering Science, University of Oxford, Oxford, UK. [3]School of Physics and Astronomy, University of Birmingham, Birmingham, UK. [4]These authors contributed equally: Joshua Feis, Sebastian Weidemann. ✉e-mail: alexander.szameit@uni-rostock.de

Methods

Experimental set-up

Our experiments are based on the propagation of light pulses in coupled optical fibre loops[28–30]. To obtain a one-dimensional photonic lattice, two optical fibre loops containing optical components are coupled by a variable beamsplitter (Agiltron). The chosen splitting ratio determines the coupling parameter β. The positions of the photonic lattice are encoded in pulse delays, and for this, the loops are chosen to have unequal optical path lengths. Here, the two roundtrip times are approximately 26,950 ns and 27,050 ns. The relative delay of 100 ns defines the width of a time bin in which the lattice positions x are encoded and, thus, approximately 270 positions can be encoded. Most of the propagation time in each loop is realized using spools of single-mode fibre (Corning Vascade LEAF EP). Each measurement starts by inserting a 50 ns pulse into the longer loop, that is, the loop that contains the spin-like components v_x^t only, via a fibre-optical beamsplitter. The initial pulse is generated via intensity modulation of a continuous-wave distributed feedback laser (JDS Uniphase, 1,550 nm) with a Mach–Zehnder modulator (SDL Integrated Optics). To further increase the signal-to-noise ratio an acousto-optical amplitude modulator (Gooch & Housego) is used. During the propagation in the loop arrangement, light is periodically split up and combined at the variable beamsplitter leading to multi-path interference between the emerging subpulses. In each roundtrip (that is, time step t), part of the light is coupled out to photodetectors (Thorlabs), enabling a measurement of $|u_x^t|^2$ and $|v_x^t|^2$. The output voltages of the photodetectors are logarithmically amplified (FEMTO, HLVA100) and subsequently acquired using an oscilloscope (Rohde & Schwarz, RTO6). With the two propagation timescales, that is, the mean roundtrip time and the relative loop delay, it is possible to map the measured pulse intensity distribution onto a double-discrete (1 + 1)-dimensional photonic lattice. To realize the gain–loss modulation, in a first step, an acousto-optical amplitude modulator (Brimrose Corporation) is added to each loop. Then, in a second step, to also realize gain and to compensate for global losses (for example, insertion loss or propagation losses in the optical fibre), an erbium-doped fibre amplifier (Thorlabs) is added to each loop. The amplifiers are optically gain-clamped by a distributed feedback laser (JDS Uniphase, 1,538 nm) that is coupled to the amplifiers input via wavelength division multiplexing couplers (AC Photonics). This continuous-wave laser signal is removed directly after the amplification process by optical bandpass filters (WL Photonics), which also reduce the level of amplified spontaneous emission. Different photonic lattices are created by applying different modulations to the variable beamsplitter and the acousto-optical modulators. The required voltage signals are generated by arbitrary waveform generators (Keysight Technologies). All optical components are designed for operation at a wavelength of 1,550 nm and use standard single-mode fibre (Corning SMF28 or comparable). The optical polarization is aligned via manual polarization controllers (Thorlabs), for instance, before passing through polarization-sensitive components.

Experimental error and power calibration

In the following, we discuss the main sources of systematic and statistical errors and their influence on the measurements. The systematic error results mainly from the limited experimental accuracy of β and g due to bias drifts and tolerances in their respective lookup tables. On the basis of calibration measurements, we assume that in our experiments the relative accuracy of both parameters is smaller than 1%. In the chosen experimental parameter regimes, such small deviations are expected to have no considerable influence, as we confirmed via numerical simulations. There is another important error contribution related to the gain–loss modulation g: constant, loop-independent excess gain or loss can easily lead to an exponential growth or decay in power as function of the time step t. This can be desired, as it does not influence the interference, but—in the case of power growth—only scales up the field distributions in each time step. However, to clearly distinguish this scaling from the topological power growth and decay, we always immediately perform a calibration measurement based on a simple homogeneous Hermitian system, that is, β = constant and $g = 0$, for which one can derive the power scaling as the deviation from constant power. The statistical error originates mainly from phase and polarization fluctuations of the pulses, which are acquired, for instance, by acoustic noise coupling to the fibre spools. However, owing to the common-path interference condition, its influence on the measurements within the shown propagation distance is negligible compared with the systematic errors. This is well reflected in very small variations in the pulse intensities upon repeating the experiment. Nevertheless, to reduce the impact of statistical errors even further, in each experiment the measured intensities are averaged over at least 20 realizations. We numerically confirmed that the resulting overall errors can explain most of the discrepancies between the experimental and the theoretical data.

Broad excitation in the time-edge state measurement

In conventional space topology, topological states are confined in space but—as eigenstates—extended in time. Conversely, time-topological states are confined in time but extended in space. To highlight this difference, we used a spatially broad excitation for measurement of the time-topological state (Fig. 3b) instead of a single-site excitation. To create the spatially broad excitation, one cannot simply insert multiple optical pulses as one would expect from the temporal encoding of neighbouring positions of the photonic lattice. To maintain the common-path interference condition and imprint a stable phase relation on all circulating pulses, the experiments must always start with a single-site excitation. Therefore, in the measurement of the time-topological state, there are 87 time steps of propagation in the fibre loops in different tailored lattices before the shown light evolution. In this time window, the broad spatial profile is created from a single optical pulse based on a non-Hermitian diffusion protocol[50,51]. This signal generation requires a phase modulator in the fibre loops, which is not shown in Fig. 2 for the sake of clarity.

Data availability

All experimental data that were used to produce the results reported in this Article are available via the Rostock University Publication Server at https://doi.org/10.18453/rosdok_id00004717 (ref. 52).

References

50. Eichelkraut, T. et al. Mobility transition from ballistic to diffusive transport in non-Hermitian lattices. *Nat. Commun.* **4**, 2533 (2013).
51. Dikopoltsev, A. et al. Observation of Anderson localization beyond the spectrum of the disorder. *Sci. Adv.* **8**, eabn7769 (2022).
52. Feis, J. et al. Data set for 'Space-time-topological events in photonic quantum walks'. *Rostock University Publication Server* https://doi.org/10.18453/rosdok_id00004717 (2025).

Acknowledgements

This work is funded by the Deutsche Forschungsgemeinschaft (DFG, German Research Foundation)—SFB 1477 'Light–Matter Interactions at Interfaces', project no. 441234705 and IRTG 2676/1-2023 'Imaging of Quantum Systems', project no. 437567992. A.S. acknowledges funding from the DFG (grants SZ 276/9-2, SZ 276/19-1, SZ 276/20-1, SZ 276/21-1 and SZ 276/27-1), the FET Open Grant EPIQUS (grant no. 899368) within the framework of the European H2020 programme for Excellent Science, as well as the Krupp von Bohlen and Halbach Foundation. J.F. acknowledges support by the Leverhulme Trust through a Study Abroad Studentship. T.S. and H.M.P. are supported by the Royal Society via grants UF160112, URF\R\221004, RGF\EA\180121 and RGF\R1\180071, and by the Engineering and Physical Sciences Research Council (grant no. EP/W016141/1).

Author contributions

J.F. and S.W. jointly developed the fundamental theory and performed the experiments. T.S. and H.M.P. developed the analytical theory of temporal interface dynamics and time-topological state profiles. A.S. and H.M.P. supervised the project. All authors contributed ideas, discussed the results and co-wrote the manuscript.

Funding

Open access funding provided by Universität Rostock.

Competing interests

The authors declare no competing interests.

Additional information

Supplementary information The online version contains supplementary material available at https://doi.org/10.1038/s41566-025-01653-w.

Correspondence and requests for materials should be addressed to Alexander Szameit.

Peer review information Nature Photonics thanks Romain Fleury and Marco Piccardo for their contribution to the peer review of this work.